Acta Scientiarum

http://periodicos.uem.br/ojs
ISSN on-line: 1807-8648
Doi: 10.4025/actascihealthsci.v46i1.64859

Influence of insertion angle and depth on the stresses produced in implants and prosthetic components - a finite element analysis

Fabiano Rito Macedo[1], Joelson Rodrigues Brum[1], Millena Barroso Oliveira[2], Douglas Teixeira da Silva[2], Walbert de Andrade Vieira[3], Igor Felipe Pereira Lima[4], Luiz Renato Paranhos[5*] and Rui Barbosa de Brito Junior[6]

[1]Universidade do Estado do Amazonas, Manaus, Amazonas, Brasil. [2]Programa de Pós-Graduação em Odontologia, Universidade Federal de Uberlândia, Uberlândia, Minas Gerais, Brasil.[3]Departamento de Odontologia Restauradora, Divisão de Endodontia, Faculdade de Odontologia de Piracicaba, Universidade Estadual de Campinas, Piracicaba, São Paulo, Brasil. [4]Departamento de Patologia Oral, Faculdade de Odontologia, Universidade Federal do Rio Grande do Sul, Porto Alegre, Rio Grande do Sul, Brasil. [5]Área de Odontologia Preventiva e Social, Faculdade de Odontologia, Universidade Federal de Uberlândia, Av. Pará, 1720,38405-320, Uberlândia, Minas Gerais, Brasil. [6]Faculdade São Leopoldo Mandic, Campinas, São Paulo, Brasil. *Author for correspondence. E-mail: paranhos.lrp@gmail.com

ABSTRACT. This study assessed the influence of different insertion angles and depths on the stress distribution in implants and prosthetic components subjected to axial and oblique loading. The study followed the Checklist for Reporting *In-vitro* Studies (CRIS) recommendations. The implant was placed in the region of element 36, according to the following models: M1 (0 mm / 0°); M2 (0 mm / 17°); M3 (0 mm / 30°); M4 (2 mm / 0°); M5 (2 mm / 17°); M6 (2 mm / 30°). All models were subjected to axial and oblique loading with an intensity of 100 N. Stress was assessed according to the Rankine and Von Mises criteria and analyzed qualitatively and quantitatively. There were minimal differences between the implants placed at bone crest height and 2 mm below it. In the external portion of the intermediates, the models angled at 30° presented higher stress concentrations under both loads. The internal part of the intermediates and the crown screw showed higher peaks as the implant angles increased. The models with inclined implants positioned below the bone crest were slightly compromised. As for the other models, the results were far from the yield point of the analyzed materials, indicating a long service life of implants and their prosthetic components in the assessed conditions.

Keywords: dental implants; dental prosthesis, implant-supported; finite element analysis.

Received on August 31, 2022
Accepted on April 03, 2023

Introduction

Implantology is a highly predictable option for replacing missing teeth functionally and esthetically (Buser, Sennerby, & Bruyn, 2017) and improving patients' oral health-related quality of life (Bugone et al., 2019). Ten-year follow-ups show success and survival rates of around 95% (Buser et al., 2012; Degidi, Nardi, & Piattelli, 2012) in treatments with implant-supported prostheses. Part of this achievement comes from research development focusing on the improvement and evolution of materials (Pellegrini, Francetti, Barbaro, & Del Fabbro, 2018) and techniques (Silveira-Neto et al., 2017).

Over the last few years, variations and clinical challenges have increasingly propelled research and, consequently, the industry (Buser et al., 2017). Implants and prosthetic components started to be developed considering the suitable adaptation of the limited anatomy of certain patients (Buser et al., 2017). For short and narrow-diameter implants, angled abutments are a reality when planning prostheses on implants (Badran et al., 2017). Moreover, the increased use of bone-level tapered implants with smaller diameters in the apical portion favors the reduction of bone graft procedures, contributing to good primary stability (Lang et al., 2007) and adaptation in immediate extraction sites and low bone density areas (Alves & Neves, 2009).

However, the biomechanical behavior of implants, intermediate abutments, and prosthetic crowns can directly affect prosthesis geometry and placement in the mouth (Tian et al., 2012). Implants at the bone level, angled at 30° under oblique loads, suggested a significant bone loss risk (Brum et al., 2020). That disagrees with one of the primary objectives of dental implant treatments, which includes achieving successful results from functional, esthetic, and phonetic standpoints and high long-term predictability and stability (Buser et al., 2017).

Thus, considering the advances in the development of new implant models and prosthetic components and the need for understanding the behavior of these materials in operational challenges, the present study assessed the influence of different insertion angles and depths on the stress distribution and service life of implants and prosthetic components subjected to axial and oblique loading, using the finite element analysis.

Material and methods

The study was submitted to the research ethics committee. It is exclusively a laboratory study, therefore dismissing the ethical analysis according to protocol #2017/0745. The article was developed according to the Checklist for Reporting *In-vitro* Studies (CRIS) recommendations (Krithikadatta, Gopikrishna, & Datta, 2014).

Achievement of three-dimensional models

The geometric models of dentate and edentulous mandibles were obtained from the online models available for free to the scientific community (Vasco, Castellano, López, & Barbosa De Las Casas, 2016). The required geometric changes were performed in CAD Solidworks 2017 software (Dassault Systems, Solidworks Corps, USA). The models were edited, and the edentulous mandible was associated with the model of tooth 36 of the dentate mandible, forming the external geometry of the future implant prosthetic crown.

Structures were created in the insertion regions of the temporal, masseter, and medial pterygoid masticatory muscles to standardize the mandibular support area. Cortical bone thickness was increased by 0.5 mm, turning 2 mm into 2.5 mm, so the total simulated implant maintained the platform anchorage in the cortical bone. The mandibular models were from a tomography of a young patient without bone loss; therefore, the posterior region of the mandible received a 2-mm bone loss model to provide an adequate crown height in all models, considering that the minimum height of the intermediates was 2.5 mm.

The three-dimensional models of implants and prosthetic components were obtained through reverse engineering with a digital caliper (Mod. 500-196-30B, Mitutoyo Sul Americana Ltda., Suzano, Brazil), a digital microscope (MV500UM-PL, Cosview Technologies Co. Ltd, Bantian, China) with a magnification of 5x ~200x, and measuring software (Miviewcap 6.0, Cosview Technologies Co. Ltd, Bantian, China) to measure component geometries and allow their modeling in Solidworks.

Sample preparation

The Straumann™ Bone-Level Tapered (BLT) Cone Morse (CM) implant (4.1 x 10 mm, Institut Straumann AG, Basel, Switzerland) with a Ti-6Al-7Nb-alloy intermediate and RC abutment (2.5 mm, Institut Straumann AG, Basel, Switzerland) was diversely placed in the region of element 36, according to the following models: M1 or control - implant perpendicular to the bone crest with the platform at crest height and a straight intermediate; M2 - implant angled at 17° to the bone crest with the platform at crest height and an intermediate angled at 17°; M3 - implant angled at 30° to the bone crest with the platform at crest height and an intermediate angled at 30°; M4 - implant perpendicular to the bone crest with the platform 2 mm below the crest and a straight intermediate; M5 - implant angled at 17° to the bone crest with the platform 2 mm below the crest and an intermediate angled at 17°; M6 - implant angled at 30° to the bone crest with the platform 2 mm below the crest and an intermediate angled at 30°. The bone crest reference was based on the buccal edge of the implant platform.

Determination of contact points

The crown of the models was made of lithium disilicate glass ceramics with a minimum thickness of 1.5 mm (IPS e.max press, Ivoclar, Vivadent, Schaan, Liechtenstein). The structure that simulated the occlusal third of antagonist teeth consisted of enamel and received contact points for axial and oblique loading. For the axial load, three round contact points with 1 mm of diameter were placed: two in the buccal cusp on the buccal and lingual sides and one in the lingual cusp. A bolus with an approximate thickness of 2 to 3 mm was placed between the crown and the antagonist structure. As for the oblique load, the points were positioned on the buccal sides of the buccal cusps.

Finite element analysis

All models were exported to Ansys Workbench V19.1 software (Ansys Inc., Canonsburg, PA, USA) to simulate finite elements. The different model elements were based on the elastic modulus and Poisson's

coefficient retrieved from the literature to represent the correct mechanical behavior of each component. All materials were isotropic, homogeneous, and linearly elastic, as shown in Table 1.

Table 1. Mechanical properties of the materials.

Material	Young's Module (GPA)	Poisson's Coefficient	References
Enamel (Antagonists)	84.1	0.33	(Mezzomo, Corso, Marczak, & Leary, 2011)
Cortical Bone	13.7	0.3	(Holmes, Diaz-Arnold, and Leary, 1996)
Espinal Bone	1.37	0.3	(Holmes et al., 1996)
Ti-6AI-7Nb Alloy (Components)	105	0.36	(AZO Materials, 2003)
Roxolid® (Implant)	124.8	0.342	(Ho, Chen, Wu, & Hsu, 2008) (MatWeb, 2016)
Lithium Disilicate Glass Ceramics (IPS e-max press)	82.3	0.22	(Trindade, Valandro, Jager, Bottino, & Kleverlaan, 2018)
Filtek Z350 XT Composite Resin (3M/ESPE, St. Paul, USA)	15.07	0.31	(Karimzadeh, Ayatollahi, & Shirazi, 2014)
Almond (Food Bolus)	0.02157	0.499	(Agrawal, Lucas, Prinz, & Bruce, 1997)

Regarding the mechanical properties of the implant alloy (Roxolid™), this study used the mean between the elastic modulus of a titanium alloy with 10% zirconia and 90% titanium and another with 20% zirconia and 80% titanium due to the absence of reliable tests for the elastic modulus of the material (Ho et al., 2008). As for Poisson's coefficient, the same titanium grade V modulus was used (MatWeb, 2016) because the materials have similar properties.

Non-linear frictional contacts with a 0.2 friction coefficient (Jörn et al., 2014) were used to simulate the contact between titanium surfaces. The same friction coefficient was used for the contact between titanium surfaces and the framework. All other contacts were simulated as sliding contacts or gap formation. The implant was considered osseointegrated.

The models were simulated in two steps. First, pre-stress was applied to the screws. A specific tool of Ansys finite elements software - "bolt pretension" - was used to improve stress standardization, allowing pre-torque stress application with a predetermined force or screw length adjustment. Thus, mesh refinement (Oatis, 2007) was verified with a temporary pre-torque in the intermediate. After adjusting the mesh, the screw load was adjusted up to a peak value of 65% of the limit of proportionality for titanium by the von Mises equivalent stress criterion, with a 1% tolerance interval. This limit was 900 MPa for the Ti-6Al-7Nb alloy (AZO Materials, 2003).

The next step included masticatory load applications, simulated with 100 N of intensity under axial and oblique loading. The first pattern or the axial load was applied with a parallel vector along the element axis in the upper portion of the structure that simulated antagonist teeth. The antagonist structure was set with frictionless supports on the sides to allow a unique gingival occlusal movement, imitating the occlusal contact. The second pattern or the oblique load was simulated with a vector toward the buccolingual aspect, forming a 30° angle with the occlusal plane. The antagonist structure was used to standardize the loading area. Rigid supports were added to the region of masticatory muscles. The simulations were non-linear to the contact.

The finite element meshes were then created with a refinement process (≤ 5%) and produced with 10-knot quadratic tetrahedral elements (solid 187), allowing to copy the irregular geometry of the analyzed models. The number of knots/elements ranged from 1087369/667132 to 1378657/854379. All models were resolved (Windows 10 64 bits, Intel I7 6800k processor, 112 Gb RAM), and the graphic and numerical plots of the data were registered, assessed, and compared by qualitative and quantitative analyses.

Stress assessments

Implants

The implants were analyzed with the Rankine criterion (Maximum Normal Stress Criterion) due to the hardening process experienced by the titanium-zirconia (TiZr) alloy used in the implant. Proportionally, the results were considered with the tensile strength of the alloy (953 MPa) (Grandin, Berner, & Dard, 2012; Osman & Swain, 2015).

Intermediate (external and internal portions) and crown screw

The components were analyzed with the von Mises criterion (Maximum Distortion Energy) due to the ductile characteristics of the titanium alloy. The results were considered with the yield point (maximum stress before plastic deformation) of 900 MPa for the Ti-6Al-7Nb alloy (AZO Materials, 2003).

Results

Implants

The stress assessment values for the implants, according to the Rankine criterion (MPa), in the axial load were M1 or control – 359.8 (38%); M2 – 423.5 (44%); M3 – 463.6 (48%); M4 – 374.2 (39%); M5 – 441.9 (46%); M6 496.8 (52%). The oblique load results were M1 or control – 370.8 (39%); M2 – 433.1 (45%); M3 - 484.8 (51%); M4 – 376.3 (39%); M5 – 417.3 (44%); M6 – 499.1 (52%).

Implants under axial and oblique loading

Figure 1 shows the results of implants under axial and oblique loading. Under axial loading, qualitatively, the peaks occurred in the region of the internal screw thread. Quantitatively, the peaks were higher before applying the load and subsequently decreased. The differences between the implants placed in the bone crest and 2 mm below were minimal. Under oblique loading, the results were similar to the axial load. Regarding the service life of implants, the peaks were far from the material tensile strength under both loads, suggesting a long service life in the analyzed conditions.

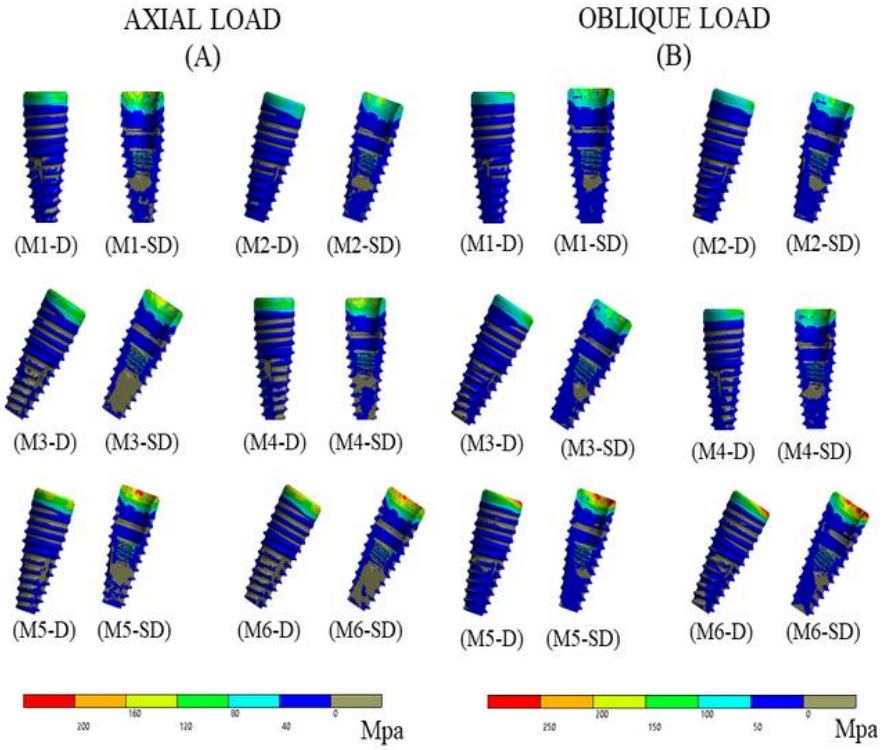

Figure 1. External distal (D) and sectioned (SD) views of implants under axial (A) and oblique (B) loading.

External portion of the intermediates

The stress assessment results according to the von Mises criterion for the axial load were M1 or control – 216.2 (24%); M2 – 360.1 (40%); M3 – 602.6 (67%); M4 – 242.3 (27%); M5 – 344.4 (38%); M6 – 618.7 (68%). The oblique load values were M1 or control - 242 (27%); M2 – 361.1 (40%); M3 – 592.1 (66%); M4 – 269.3 (32%); M5 – 345.3 (38%); M6 – 607.5 (67%).

External portion of intermediates under axial and oblique loading

Figure 2 shows the results of the external portion of intermediates under axial and oblique loading. In the axial load, qualitatively, the peaks of models M1 and M4 occurred in the conical region of implant contact.

However, the other models peaked on the upper threads of intermediates, on the wear side to pass the screw that joins the intermediate to the implant. Quantitatively, the peaks were lower in implants M1 and M4. The models with 30° angles presented higher stress concentrations than those at 17°. The oblique load results were similar to the axial load. Regarding the service life of the external portion of intermediates, the peaks were far from the material yield point under axial and oblique loading, showing a long service life in the analyzed conditions.

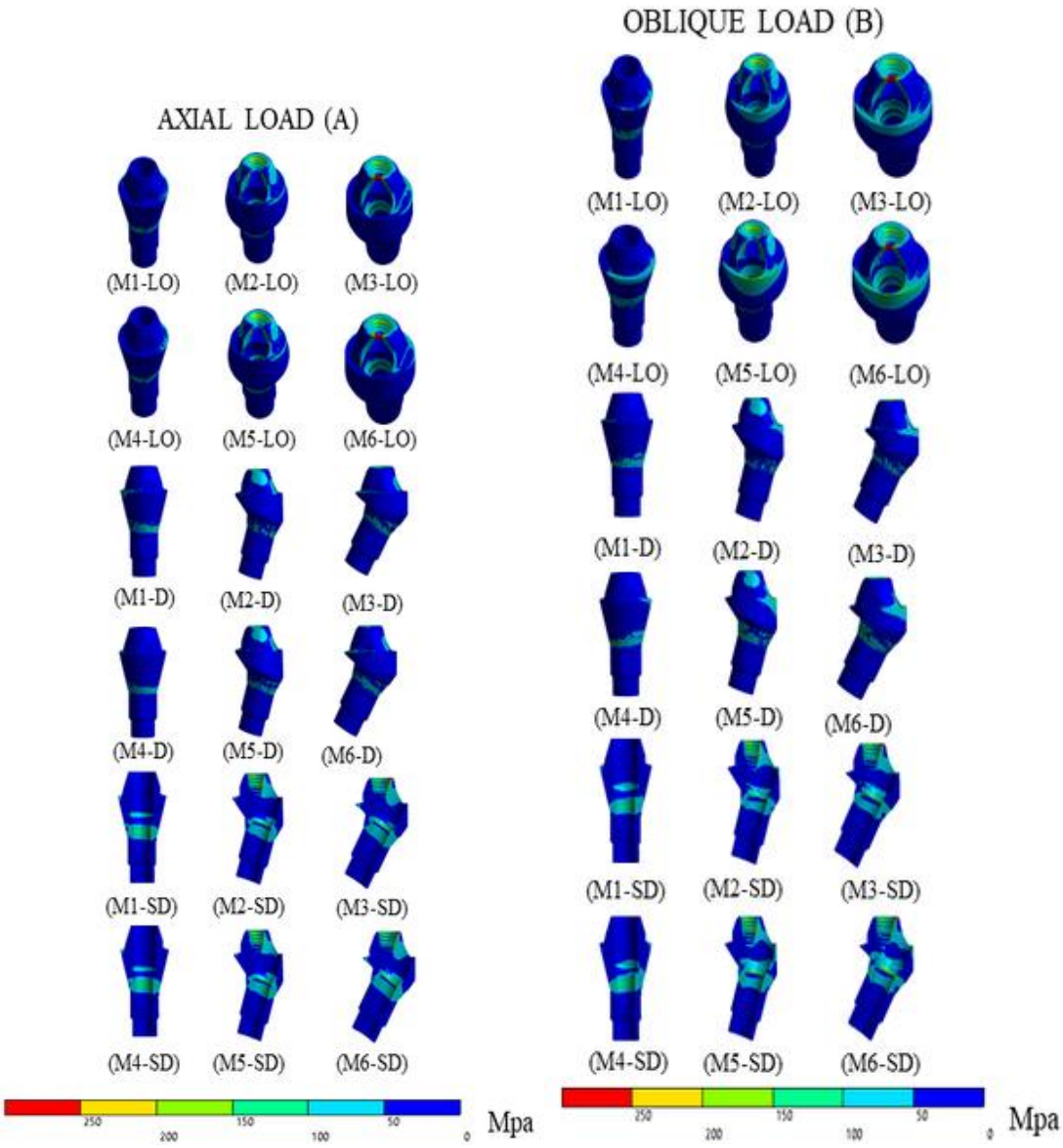

Figure 2. Lingual-occlusal (LO), external distal (D), and sectioned (SD) views of the external portion of intermediates under axial (A) and oblique (B) loading.

Internal portion of the intermediates

Stress assessment results according to the von Mises criterion for the axial load were M1 or control – 481.4 (53%); M2 – 520.6 (58%); M3 – 433.9 (48%); M4 – 427 (47%); M5 – 457 (51%); M6 – 470.6 (52%). The oblique load values were M1 or control - 482.2 (53%); M2 – 494.3 (55%); M3 – 551.2 (61%); M4 – 444.7 (49%); M5 – 509.6 (56%); M6 – 590.3 (65%).

Internal portion of intermediates under axial loading

Figure 3 shows the results of the internal portion of intermediates under axial loading. Qualitatively, the peaks occurred in the region of the lower threads. As for the quantitative aspects, the lower peaks occurred in model M2 and the higher ones in model M5.

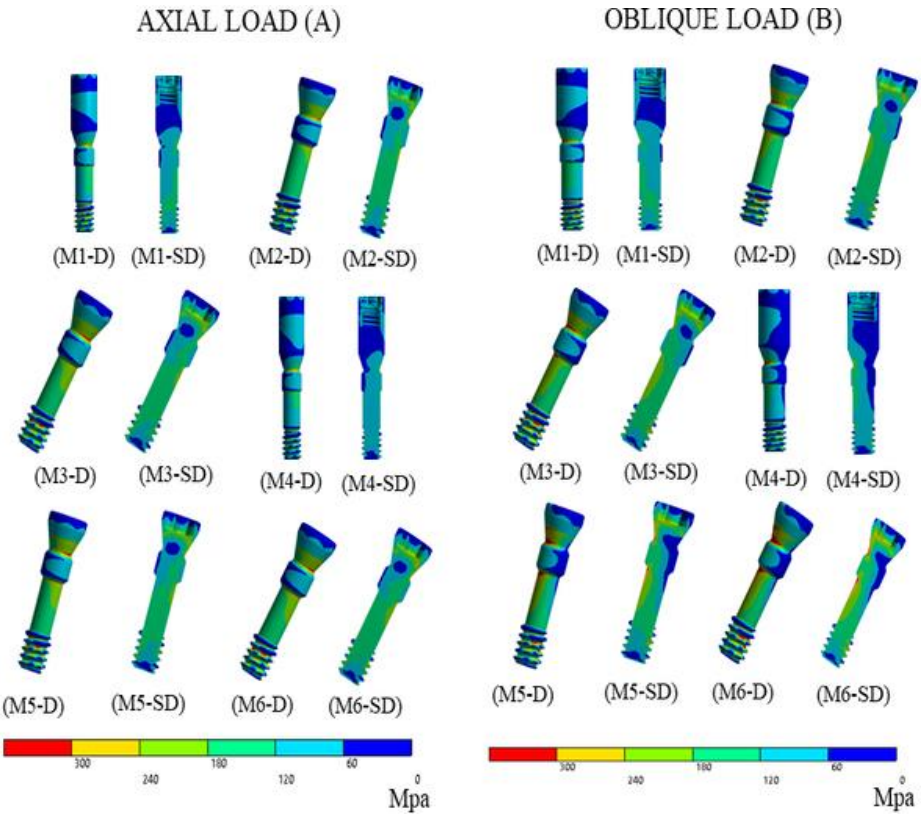

Figure 3. External distal (D) and sectioned (SD) views of the internal portion of intermediates under axial (A) and oblique (B) loading.

Internal portion of intermediates under oblique loading

Figure 3 shows the results of the internal portion of intermediates under oblique loading. Qualitatively, the peaks of models M1 to M4 occurred in the thread angles. Models M5 and M6 peaked in the lower region of the screw cone (the connection between the screw and the intermediate).

Quantitatively, there was a tendency for higher peaks as implant angles increased. In turn, the stress oscillation in the peaks of the different models, responsible for the fatigue phenomenon, was proportionally higher in implants installed 2 mm below the bone crest, as shown in Table 2. The highest peaks were far from the titanium yield point, suggesting a long service life of the components in the analyzed conditions, except for implant models placed 2 mm below the bone crest, in which service life seemed shorter.

Table 2. Stress peaks in the internal portion of intermediates under oblique loading, according to the von Mises criterion (in MPa), and the percentage relative to the yield point of the Ti-6Al-7Nb alloy.

Models	Values
Model M1 (0 mm / 0°)	582.82 – 482.2 = 100.62 / 11%
Model M2 (0 mm / 17°)	585.49 – 494.3 = 91.19 / 10%
Model M3 (0 mm / 30°)	581.28 – 551.2 = 30.08 / 3%
Model M4 (2 mm / 0°)	583.43 – 444.7 = 138.73 / 15%
Model M5 (2 mm / 17°)	343.25 – 509.6 = (-166.35) / 18%
Model M6 (2 mm / 30°)	406.35 – 590.3 = (-183.95) / 20%

Crown screw

Stress assessment results according to the von Mises criterion for the axial load were M1 or control – 529.9 (59%); M2 – 548.7 (61%); M3 – 525.9 (58%); M4 – 505.5 (56%); M5 – 546 (60%); M6 – 527.3 (58%). The oblique load values were M1 or control - 509.9 (56%); M2 – 583.8 (65%); M3 – 595.7 (66%); M4 – 512.4 (57%); M5 – 587.4 (65%); M6 – 625.8 (69%).

Crown screw under axial loading

Figure 4 shows the crown screw results under axial loading. Qualitatively, the peaks occurred in the first screw threads. Models M1 and M4 showed high stresses along the threads, and the other models had more

concentrated stresses. As for inclined implant models, the peaks were concentrated in the buccal aspect. Considering the analyzed variations, quantitatively, the results were close to a maximum of 5% between M2 and M4. As for service life, all the results were far from the material yield point, indicating a long service life in the analyzed conditions.

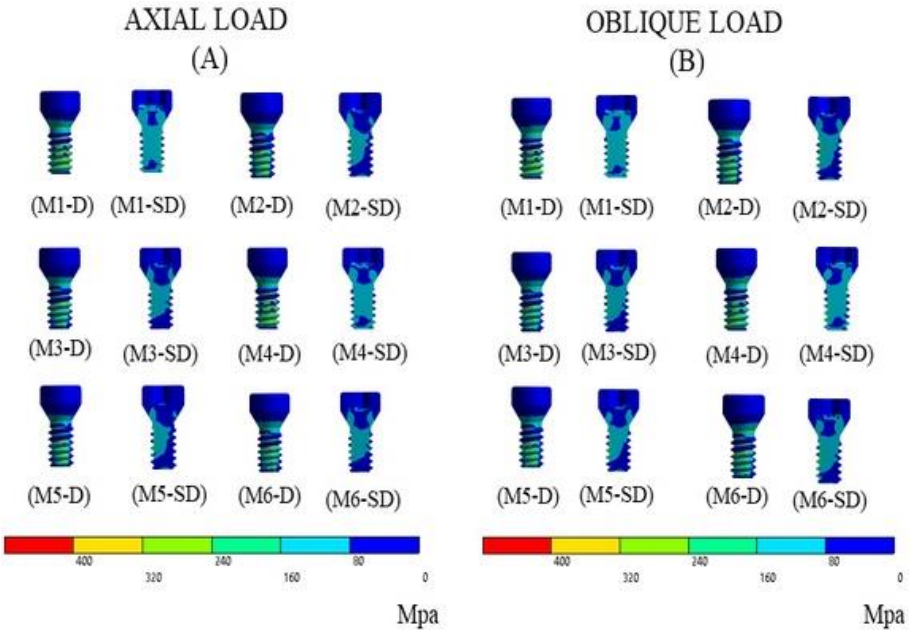

Figure 4. External distal (D) and sectioned (SD) views of crown screws under axial (A) and oblique (B) loading.

Crown screw under oblique loading

Crown screw results under oblique loading, qualitatively, showed peaks in the first screw threads, similar to the axial load. Inclined models presented the highest peaks, indicating a slightly shorter service life in these implant models, as shown in Figure 4.

Discussion

The present study investigated the influence of different insertion angles and depths on the stress levels distributed in implants, prosthetic intermediates, and crown screws and the impacts on the service life of these structures. Implants and prosthetic intermediates angled at 17° and 30° and straight were simulated. The implants were placed at the bone crest level and 2 mm below. Six models were created, with M1 (0° / 0 mm) as the control, and the Straumann™ Bone-Level Tapered (BLT) implant was used (Dard et al., 2016).

Under axial and oblique loading, the stress peak differences between implants placed at crest height and 2 mm below were minimal. That is because the peaks occurred in the region of internal screw threads, minimizing the influence of bone insertion on the received stresses. Thus, the highest stress levels occurred in the angled implant models M5 and M6 under both loads. The findings corroborate the results of a recent study that showed more consequences associated with the group of implants angled at 17° and 30° (Brum et al., 2020).

Regarding the external portion of intermediates under axial and oblique loading, models M1 and M4 presented stress peaks in the conical region of implant contact. This area is usually susceptible to higher compression due to the pre-stress of screws associated with the masticatory load. When using the concept of a reduced abutment platform, most of the stress was located in the platform-abutment connection, and the oblique load was responsible for the highest stress level (Tabata, Rocha, Barão, & Assunção, 2011). The results for axial and oblique loads were similar in the present study.

The intermediates in model M6 (30°) presented higher stress concentrations than implants in model M5 (17°). Regardless, the peaks were far from the material yield point, showing a long service life of the structure in the analyzed conditions. Moreover, angled abutments were efficient considering the impossibility of installing implants in the optimal axial position, which can decrease and improve stress distributions in the peri-implant bone tissue (Chu, Huang, Hsu, & Fuh, 2012; Brum et al., 2020).

As for the internal portion of intermediates under oblique loading, quantitatively, the highest peaks also occurred in angled models. However, the implants installed 2 mm below the bone crest showed the highest stress oscillation responsible for fatigue, compromising the service life of these models under oblique loading. It is worth noting that the implants used in the study were bone-level tapered implants (Dard et al., 2016), justifying the influence of unsatisfactory results on the models installed 2 mm below this level.

Crown screw results under axial loading in models M1 (0°) and M4 (0°) showed stresses distributed along the threads, and in the inclined models M2 (17°), M3 (30°), M5 (17°), and M6 (30°), the regions of high stress were more concentrated on the buccal side due to the wear of intermediates for passing the implant screw. The present study used lithium-disilicate glass ceramicto simulate implant-supported crowns. The literature shows lower stress toward the retention screw of the prosthesis in crowns made of porcelain with zirconia coping than in other ceramic crowns cast in different coping materials (Gomes, Barão, Rocha, Almeida, & Assunção, 2011).

Still regarding axial loading, the quantitative results were similar, with a maximum variation of 5% between M2 and M4, showing that the angle compensation of intermediates in the inclined models approaches the prosthesis screw component to the results of the straight models (Tian et al., 2012). Screws under oblique loading showed peaks similar to the axial load, with a difference in flexural behavior caused by the oblique load in angled models, indicating a slightly shorter service life in inclined implant models. The results were similar for the forces applied, and the oblique load showed higher intensity and stress distribution than the axial load (Tabata et al., 2011).

The finite element analysis results helped to understand the biomechanical behavior of an implant system available in the market. Thus, further research is required, addressing other implant systems, intermediate abutments, and crowns for better indications and decreased risks of clinical failure.

The present study is not free of limitations. Standing out among them is the inability of the finite element analysis model to simulate the torsion stresses in the contact area between the screw thread and the implant relative to the contact area of the implant head and the intermediate (SKF, 2001). However, a bolus was simulated between the occlusal third of the ceramic crown and the antagonist structure in enamel, allowing a suitable simulation closer to the clinical reality of the studied models.

Conclusion

The applied stressesslightly compromised inclined models and those placed below the bone crest. As for the other models, the results were far from the yield point of the analyzed materials, indicating a long service life of implants and their prosthetic components in the assessed conditions.

Acknowledgments

This study was partially financed by CAPES (Coordination for the Improvement of Higher Education Personnel - Brazil) – Finance Code 001. We also appreciate the support of CNPq (National Council of Scientific and Technological Development - Brazil) and FAPEMIG (Minas Gerais Research Foundation - Brazil).

References

Agrawal, K. R., Lucas, P. W., Prinz, J. F., & Bruce, I. C. (1997). Mechanical properties of foods responsible for resisting food breakdown in the human mouth. *Archives of Oral Biology, 42*(1), 1-9. DOI: https://doi.org/10.1016/S0003-9969(96)00102-1

Alves, C. C., & Neves, M. (2009). Tapered implants: from indications to advantages. *The International Journal of Periodontics & Restorative Dentistry, 29*(2), 161-167.

AZO Materials. (2003). *Titanium Alloys - Ti6Al7Nb Properties and Applications*. Retrieved from https://www.azom.com/article.aspx?ArticleID=2064.

Badran, Z., Struillou, X., Strube, N., Bourdin, D., Dard, M., Soueidan, A., & Hoornaert, A. (2017). Clinical performance of narrow-diameter titanium-zirconium implants: a systematic review. *Implant Dentistry, 26*(2), 316-323. DOI: https://doi.org/10.1097/ID.0000000000000557

Brum, J. R., Macedo, F. R., Oliveira, M. B., Paranhos, L. R., Brito-Júnior, R. B., & Ramacciato, J. C. (2020). Assessment of the stresses produced on the bone implant/tissue interface to the different insertion

angulations of the implant-a three-dimensional analysis by the finite elements method. *Journal of Clinical and Experimental Dentistry, 12*(10), e930-e937. DOI: https://doi.org/10.4317/jced.57387

Bugone, É., Vicenzi, C. B., Cardoso, M. Z., Berra, L., De Carli, J. P., Franco, A., & Paranhos, L. R. (2019). The impact of oral rehabilitation with implants in nutrition and quality of life: A questionnaire-based survey on self-perception. *Journal of Clinical and Experimental Dentistry, 11*(5), e470. DOI: https://doi.org/10.4317/jced.55647

Buser, D., Janner, S. F., Wittneben, J. G., Brägger, U., Ramseier, C. A., & Salvi, G. E. (2012). 10-year survival and success rates of 511 titanium implants with a sandblasted and acid-etched surface: a retrospective study in 303 partially edentulous patients. *Clinical Implant Dentistry and Related Research, 14*(6), 839-851. DOI: https://doi.org/10.1111/j.1708-8208.2012.00456.x

Buser, D., Sennerby, L., & De Bruyn, H. (2017). Modern implant dentistry based on osseointegration: 50 years of progress, current trends and open questions. *Periodontology 2000, 73*(1), 7-21. DOI: https://doi.org/10.1111/prd.12185

Chu, C. M., Huang, H. L., Hsu, J. T., & Fuh, L. J. (2012). Influences of internal tapered abutment designs on bone stresses around a dental implant: Three-dimensional finite element method with statistical evaluation. *Journal of Periodontology, 83*(1), 111-118. DOI: https://doi.org/10.1902/jop.2011.110087

Dard, M., Kuehne, S., Obrecht, M., Grandin, M., Helfenstein, J., & Pippenger, B. E. (2016). Integrative performance analysis of a novel bone level tapered implant. *Advances in Dental Research, 28*(1), 28-33. DOI: https://doi.org/10.1177/0022034515624443

Degidi, M., Nardi, D., & Piattelli, A. (2012). 10-year follow-up of immediately loaded implants with TiUnite porous anodized surface. *Clinical Implant Dentistry and Related Research, 14*(6), 828-838. DOI: https://doi.org/10.1111/j.1708-8208.2012.00446.x

Gomes, É. A., Barão, V. A., Rocha, E. P., Almeida, É. O., & Assunção, W. G. (2011). Effect of Metal-Ceramic or All-Ceramic Superstructure Materials on Stress Distribution in a Single Implant-Supported Prosthesis: Three-Dimensional Finite Element Analysis. *The International Journal of Oral & Maxillofacial Implants, 26*(6), 1202-1209.

Grandin, H. M., Berner, S., & Dard, M. (2012). A review of titanium zirconium (TiZr) alloys for use in endosseous dental implants. *Materials, 5*(8), 1348-1360. DOI: https://doi.org/10.3390/ma5081348

Holmes, D. C., Diaz-Arnold, A. M., & Leary, J. M. (1996). Influence of post dimension on stress distribution in dentin. *The Journal of Prosthetic Dentistry, 75*(2), 140-147. DOI: https://doi.org/10.1016/S0022-3913(96)90090-6

Ho, W. F., Chen, W. K., Wu, S. C., & Hsu, H. C. (2008). Structure, mechanical properties, and grindability of dental Ti–Zr alloys. *Journal of materials science: Materials in medicine, 19*(10), 3179-3186. DOI: https://doi.org/10.1007/s10856-008-3454-x

Jörn, D., Kohorst, P., Besdo, S., Rücker, M., Stiesch, M., & Borchers, L. (2014). Influence of lubricant on screw preload and stresses in a finite element model for a dental implant. *The Journal of Prosthetic Dentistry, 112*(2), 340-348. DOI: https://doi.org/10.1016/j.prosdent.2013.10.016

Karimzadeh, A., Ayatollahi, M. R., & Shirazi, H. A. (2014). Mechanical properties of a dental nano-composite in moist media determined by nano-scale measurement. *International Journal of Materials, Mechanics and Manufacturing, 2*(1), 67-72. DOI: http://dx.doi.org/10.18178/IJMMM

Krithikadatta, J., Gopikrishna, V., & Datta, M. (2014). CRIS Guidelines (Checklist for Reporting In-vitro Studies): A concept note on the need for standardized guidelines for improving quality and transparency in reporting in-vitro studies in experimental dental research. *Journal of Conservative Dentistry: JCD, 17*(4), 301-304. DOI: https://doi.org/10.4103/0972-0707.136338

Lang, N.P., Tonetti, M.S., Suvan, J.E., Pierre Bernard, J., Botticelli, D., Fourmousis, I., ...Weber, H.-P. (2007). Immediate implant placement with transmucosal healing in areas of aesthetic priority: A multicentre randomized-controlled clinical trial I. Surgical outcomes. *Clinical Oral Implants Research, 18*(2), 188-196. DOI: https://doi.org/10.1111/j.1600-0501.2006.01371.x

MatWeb. (2016). *Material Property Data. MatWeb Titanium Ti-6Al-4V (Grade 5), Annealed*. Retrieved from https://www.matweb.com/search/DataSheet.aspx?MatGUID=10d463eb3d3d4ff48fc57e0ad1037434

Mezzomo, L. A., Corso, L., Marczak, R. J., & Rivaldo, E. G. (2011). Three-dimensional FEA of effects of two dowel-and-core approaches and effects of canal flaring on stress distribution in endodontically treated

teeth. *Journal of Prosthodontics: Implant, Esthetic and Reconstructive Dentistry, 20*(2), 120-129. DOI: https://doi.org/10.1111/j.1532-849X.2010.00669.x

Oatis, D. (2007). Analyzing bolt pretension in the ANSYS Workbench Platform. *ANSYS Advantage, 1*(4), 28-29.

Osman, R. B., & Swain, M. V. (2015). A critical review of dental implant materials with an emphasis on titanium versus zirconia. *Materials, 8*(3), 932-958. DOI: https://doi.org/10.3390/ma8030932

Pellegrini, G., Francetti, L., Barbaro, B., & Del Fabbro, M. (2018). Novel surfaces and osseointegration in implant dentistry. *Journal of Investigative and Clinical Dentistry, 9*(4). DOI: https://doi.org/10.1111/jicd.12349

Silveira-Neto, N., Flores, M. E., De Carli, J. P., Costa, M. D., Matos, F. D. S., Paranhos, L. R., & Linden, M. S. S. (2017). Peri-implant assessment via cone beam computed tomography and digital periapical radiography: an ex vivo study. *Clinics*, 72, 708-713. DOI: https://doi.org/10.6061/clinics/2017(11)10

SKF, G. (2001). Bolt-tightening handbook. *In Technologies SLMP, Montigny-le-Bretinneux*. France.

Tabata, L. F., Rocha, E. P., Barão, V. A. R., & Assunção, W. G. (2011). Platform switching: biomechanical evaluation using three-dimensional finite element analysis. *International Journal of Oral & Maxillofacial Implants, 26*(3), 482-491.

Tian, K., Chen, J., Han, L., Yang, J., Huang, W., & Wu, D. (2012). Angled abutments result in increased or decreased stress on surrounding bone of single-unit dental implants: a finite element analysis. *Medical Engineering & Physics, 34*(10), 1526-1531. DOI: https://doi.org/10.1016/j.medengphy.2012.10.003

Trindade, F. Z., Valandro, L. F., Jager, N., Bottino, M. A., & Kleverlaan, C. J. (2018). Elastic properties of lithium disilicate versus feldspathic inlays: effect on the bonding by 3D finite element analysis. *Journal of Prosthodontics, 27*(8), 741-747. DOI: https://doi.org/10.1111/jopr.12550

Vasco, M. A., Castellano, M. D., López, J. B., & De Las Casas, E. B. (2016). Utilização de tomografias computadorizadas de baixa resolução para construção de modelos geométricos detalhados de mandíbulas com e sem dentes. *Revista Internacional de Métodos Numéricos para Cálculo y Diseño en Ingeniería, 32*(1), 1-6. DOI: https://doi.org/10.1016/j.rimni.2014.09.003